Success Probability of Millimeter-Wave D2D Networks with Heterogeneous Antenna Arrays

Na Deng, Yi Sun
School of Information & Communication Engineering
Dalian University of Technology
Dalian, Liaoning, 116024, China
Email:{dengna,lslwf}@dlut.edu.cn

Martin Haenggi
Dept. of Electrical Engineering
University of Notre Dame
Notre Dame, IN, 46556, USA
Email:mhaenggi@nd.edu

***Abstract*—This paper focuses on the success probability (or, equivalently, the signal-to-interference-plus-noise ratio (SINR) distribution) at the typical receiver in millimeter wave (mm-wave) device-to-device (D2D) networks. Unlike earlier works, we consider a more general and realistic case where devices in the network are equipped with heterogeneous antenna arrays so that the concurrent transmission beams are varying in width. Specifically, we first establish a general and tractable framework for the target network with Nakagami fading and directional beamforming. Next, we investigate the interactions among beams with different widths and their sensitivities to the adopted model for the antenna pattern. In addition, to show the impact of heterogeneous antenna arrays on the link performance, we derive the success probability of the typical receiver as well as its bounds to get deep insights on the performance of the network.**

I. Introduction

The proliferation of high-speed multi-media applications and high-end devices exacerbates the demand for high data rate services. According to the latest visual network index (VNI) report from Cisco [1], the global mobile data traffic will increase nearly sevenfold between 2016 and 2021, reaching 49.0 exabytes per month by 2021, wherein more than three-fourths will be video. The need for greater capacity, and hence greater spectrum utilization, has very recently led to the advent of millimeter wave (mm-wave) device-to-device (D2D) communications to efficiently use the large bandwidth (multiple gigahertz).

However, this emerging technology is still in its infancy, and it is unclear what benefits and challenges it will bring. It is clear that mm-wave D2D communication is more complicated than sub-6 GHz D2D and mm-wave cellular communications. Firstly, the narrow beam width of mm-wave and the relatively low antenna height (compared with that of BSs) render the mm-wave D2D communication even more vulnerable to blockages. Secondly (and more importantly), different from the cellular BSs that are usually equipped with homogeneous antenna arrays (namely the same number of antennas), the devices have their inherent diverse properties and random locations, which means devices in the network cannot be expected to be equipped with the same number of antennas and located in a well-planned manner. Therefore, in this paper, we will present a comprehensive investigation on the heterogeneous mm-wave D2D networks and obtain useful insights for the further development of mm-wave D2D communications.

Although mm-wave devices offer several potential advantages for D2D networks, there has been limited application of stochastic geometry to study the potential performance of mm-wave D2D networks incorporating key features of the mm-wave band. The primary related works are [2] and [3]: the former approximated the directional beamforming by a sectored model with the assumption of homogeneous antenna arrays and blockage effects but considered a finite number of interferers in a finite network region; while the latter proposed two more accurate antenna pattern models with the same assumption in [2]. In contrast, our prior work in [4] used stochastic geometry to provide a fine-grained performance analysis of mm-wave D2D networks in terms of the *meta distribution*, and it also considered the simplified sectored model for the antenna pattern with uniform antenna array. To the best of our knowledge, the effect of the heterogeneity of the antenna arrays on the potential performance of mm-wave D2D networks has not been studied in conjunction with accurate approximations for the actual antenna pattern. In this work, we will fill this gap with new analytical results of the success probability in a stochastic geometry framework.

II. Network Model

It is assumed that the transmitters belonging to the k-th tier are distributed uniformly in the two-dimensional Euclidean space $\mathbb{R}^2$ according to a homogeneous PPP Φ_k of density λ_k and operate at a constant transmit power μ_k. For all $j \neq i$, Φ_j and Φ_i are independent. The ALOHA channel access scheme is adopted, i.e., in each time slot, D2D transmitters in Φ_k independently transmit with probability q_k. Accordingly, the distribution of the devices in mm-wave D2D networks is defined as $\Phi = \bigcup_{k=1}^{K} \Phi_k$ with density $\lambda = \sum_{k=1}^{K} \lambda_k$. Each transmitter is assumed to have a dedicated receiver at distance r_0 in a random orientation, i.e., the D2D users form a K-tier *Poisson bipolar network* [5, Def. 5.8]. Without loss of generality, we consider a receiver at the origin that attempts to receive from an additional transmitter located at $(r_0, 0)$. Due to Slivnyak's theorem [5, Thm. 8.10], this receiver becomes the typical receiver under expectation over the (overall) PPP. To analyze the typical D2D receiver belonging to the k-th tier, we further condition on that receiver at the origin to belong to the k-th tier with parameters (such as transmit power, number of antennas, etc.) chosen from that tier.

A. Blockage and Propagation Model

The signal path can be either LOS/unblocked or NLOS/blocked, each with a different path loss exponent. The generalized LOS ball model [6] is adopted to capture the blockage effect in mm-wave communication, which was verified to be as accurate as the empirical 3GPP blockage model by experiments in [7]. Specifically, the LOS probability of the signal path between two nodes with separation d is

$$P_{\mathrm{LOS}}(d) = p_{\mathrm{L}} \mathbf{1}(d < R), \tag{1}$$

where $\mathbf{1}(\cdot)$ is the indicator function, R is the maximum length of a LOS channel, and $p_{\mathrm{L}} \in [0, 1]$ is the LOS probability if $d \le R$. Let $\alpha_{k,\mathrm{L}}$ and $\alpha_{k,\mathrm{N}}$ denote the path loss exponents of LOS and NLOS paths belonging to the k-th tier, respectively. Typical values for mm-wave path loss exponents can be found in [8] with approximated ranges of $\alpha_{k,\mathrm{L}} \in [1.9, 2.5]$ and $\alpha_{k,\mathrm{N}} \in [2.5, 4.7]$.

B. Directional Beamforming Model

We assume that the transmitters belonging to k-th tier are equipped with a uniform linear array (ULA) composed of N_k antenna elements to perform directional beamforming and their corresponding receivers have a single antenna. It is also assumed that the transmitter knows the direction to the receiver so that it can point its AoD at its receiver perfectly to obtain the maximum power gain. Recently, an accurate approximation termed cosine antenna pattern was proposed in [3], which is shown to constitute a desirable trade-off between accuracy and tractability in the performance analysis of mm-wave networks. This antenna pattern approximation is based on the cosine function with the antenna gain function

$$G_k(\varphi) = \begin{cases} N_k \cos^2\left(\frac{\pi N_k}{2}\varphi\right) & \text{if } |\varphi| \le 1/N_k \\ 0 & \text{otherwise,} \end{cases} \tag{2}$$

where $\varphi = \frac{d_{\mathrm{t}}}{\varrho}\cos\phi$ is the cosine direction corresponding to the AoD ϕ of the transmit signal, which is termed as the *spatial AoD*, with d_{t} and ϱ representing the antenna spacing and wavelength, respectively. The antenna spacing d_{t} is usually set to be half-wavelength to enhance the directionality of the beam and avoid grating lobes; the spatial AoD φ is assumed to be uniformly distributed in $[-0.5, 0.5]$, and thus the spatial AoD from an interferer to the typical receiver is also uniformly distributed in $[-0.5, 0.5]$, as proven in [3]. While for the mostly used sectored antenna pattern, the array gains within the half-power beamwidth are assumed to be the maximum power gain, and the array gains corresponding to the remaining AoDs are approximated to be the first minor maximum gain of the actual antenna pattern. Although this simple approximation is highly tractable, it causes significant deviations from the actual performance, especially when there are differences in the number of antennas among different devices in the network.

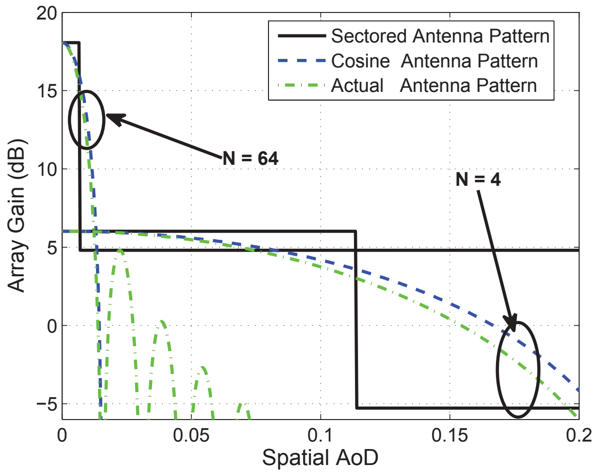

Fig. 1. Visualization of three different antenna patterns for $N = 4$ and $N = 64$.

In Fig. 1, we compare the cosine antenna pattern, the sectored antenna pattern, as well as the actual antenna pattern [9]. From the actual antenna pattern, we can observe that the first side lobe gain of $N = 64$ is within 1 dB of the main lobe gain of $N = 4$ but limited in a quite small range of AoDs, which means the side lobe leakage causes high interference to other devices in a very narrow range of directions. For the sectored pattern, the array gains corresponding to all the directions outside the main lobe are assumed to be equal to the first side lobe gain of the actual pattern. Obviously, this approximation leads to deviation from the actual antenna pattern and exaggerates the effect of side lobe leakage. The larger the number of antennas, the greater the deviations. It is even worse for networks where different kinds of devices are likely to be equipped with different numbers of antennas. Thus, taking both accuracy and tractability into consideration, the cosine antenna pattern is adopted in the following analysis, which makes it possible to investigate the impact of heterogeneous antenna arrays on the performance.

C. SINR Analysis

We assume that the desired link between the transmitter-receiver pair is in the LOS condition with deterministic path loss $r_0^{-\alpha_{k,\mathrm{L}}}$ given that the typical receiver belongs to the k-th tier. In fact, if the receiver was associated with a NLOS transmitter, the link would quite likely be in outage due to the severe propagation loss and high noise power at mm-wave bands as well as the fact that the interferers can be arbitrarily close to the receiver. Different path loss exponents are applied to the cases of LOS and NLOS paths. We denote by $\ell_k(x)$ the random path loss function associated with the interfering transmitter location $x \in \Phi_k$, given by

$$\ell_k(x) = \begin{cases} (\max\{d_0, |x|\})^{-\alpha_{k,\mathrm{L}}} & \text{w.p. } P_{\mathrm{LOS}}(|x|) \\ (\max\{d_0, |x|\})^{-\alpha_{k,\mathrm{N}}} & \text{w.p. } 1 - P_{\mathrm{LOS}}(|x|), \end{cases} \tag{3}$$

where all $\ell_k(x)_{x\in\Phi_k}$ are independent. In addition to the distance-dependent path loss, we assume independent Nakagami fading for each path, which is a sensible model given the LOS-dependent mm-wave scenarios. Different Nakagami fading parameters $M_{k,\mathrm{L}}$ and $M_{k,\mathrm{N}}$ are assumed for LOS and NLOS paths in the k-th tier, where $M_{k,\mathrm{L}}$ and $M_{k,\mathrm{N}}$ are positive integers. The power fading coefficient between node $x \in \Phi_k$ and the origin is denoted by h_x, which follows a gamma distribution $\mathrm{Gamma}(M, \frac{1}{M})$ with $M \in \{M_{k,\mathrm{L}},\ M_{k,\mathrm{N}}\}$, and all h_x are mutually independent and also independent of the point process. For the typical receiver, the interferers outside the LOS ball are NLOS and thus can be ignored due to the severe path loss over the large distance (at least R). As a result, the analysis for the network originally composed by the multi-tier PPPs reduces to the analysis of a finite network region, namely the disk of radius R centered at the origin.

Based on this model, the interference from tier k at the origin is

$$I_k = \sum_{x\in\Phi_k} \mu_k G_k(\varphi_x) h_x \ell_k(x) B_k(x), \tag{4}$$

where $G_k(\varphi_x)$ is the directional antenna gain function with spatial AoD φ_x following (2), and $B_k(x)$ is a Bernoulli variable with parameter q_k to indicate whether x transmits a message to its receiver. Due to the incorporation of the blockages, the LOS transmitters belonging to the k-th tier with LOS propagation to the typical receiver form a PPP $\Phi_{k,\mathrm{L}}$ with density $p_\mathrm{L}\lambda_k$, while $\Phi_{k,\mathrm{N}}$ with density $p_\mathrm{N}\lambda_k$ is the transmitter set with NLOS propagation, where $p_\mathrm{L} + p_\mathrm{N} = 1$ such that $\Phi_k = \Phi_{k,\mathrm{L}} \cup \Phi_{k,\mathrm{N}}$. Then, the interference from tier k can be rewritten as

$$\begin{aligned} I_k &= I_{k,\mathrm{L}} + I_{k,\mathrm{N}} \\ &= \sum_{s\in\{\mathrm{L,N}\}} \sum_{x\in\Phi_{k,s}} \mu_k G_k(\varphi_x) h_x \ell_k(x) B_k(x). \end{aligned} \tag{5}$$

Without loss of generality, the noise power is set to one. Conditioning on that the typical receiver belongs to the k-th tier, the corresponding receiver SINR, denoted as SINR_k, is then given by

$$\mathrm{SINR}_k \triangleq \frac{S_k}{1+I} = \frac{\mu_k N_k h_{x_0} r_0^{-\alpha_{k,\mathrm{L}}}}{1+\sum\limits_{i\in[K]}\sum\limits_{x\in\Phi_i} \mu_i G_i(\varphi_x) h_x \ell_i(x) B_i(x)}, \tag{6}$$

where $[K] \triangleq \{1, 2, ..., K\}$.

III. Analysis of Success Probability

A. Exact Results

Our first result in this section is an exact expression for the success probability $\mathbb{P}(\mathrm{SINR} > \theta)$ conditioning on the typical receiver belonging to tier k.

Theorem 1. *Letting $\epsilon_k = \frac{M_{k,\mathrm{L}} r_0^{\alpha_{k,\mathrm{L}}}}{\mu_k N_k}$, the link success probability of the typical active device belonging to the k-th tier equipped with N_k antennas, denoted by $P_k(\theta)$, is given by*

$$P_k(\theta) = \sum_{m=0}^{M_{k,\mathrm{L}}-1} \frac{(-u)^m}{m!} \mathcal{L}^{(m)}(u)|_{u=\theta\epsilon_k}, \tag{7}$$

where $\mathcal{L}(u) = \exp(\eta(u))$, the superscript '$(m)$' stands for the m-th derivative of $\mathcal{L}(u)$, and

$$\eta(u) = -u - \sum_{i\in[K]}\sum_{s\in\{\mathrm{L,\,N}\}} p_s \lambda_i q_i \frac{2}{N_i}\Bigg(\pi R^2 - \int_0^R\int_0^{\frac{\pi}{2}} \frac{M_{i,s}^{M_{i,s}} 4r\mathrm{d}x\mathrm{d}r}{\left(M_{i,s}+u\mu_i N_i \cos^2 x \max\{r, d_0\}^{-\alpha_{i,s}}\right)^{M_{i,s}}}\Bigg). \tag{8}$$

$\mathcal{L}^{(m)}(u)$ is given recursively by

$$\mathcal{L}^{(m)}(u) = \sum_{n=0}^{m-1} \binom{m-1}{n} \eta^{(m-n)}(u)\mathcal{L}^{(n)}(u), \tag{9}$$

where the n-th derivative of $\eta(u)$ follows

$$\eta^{(n)}(u) = -\mathbf{1}(n=1) + \sum_{i\in[K]}\sum_{s\in\{\mathrm{L,\,N}\}} p_s \lambda_i q_i \frac{8\Gamma(M_{i,s}+n) M_{i,s}^{M_{i,s}}}{N_i \Gamma(M_{i,s})} \times \int_0^R\int_0^{\frac{\pi}{2}} \frac{(-\mu_i N_i \cos^2 x \max\{r, d_0\}^{-\alpha_{i,s}})^n r\mathrm{d}x\mathrm{d}r}{\left(M_{i,s}+u\mu_i N_i \cos^2 x \max\{r, d_0\}^{-\alpha_{i,s}}\right)^{M_{i,s}+n}}. \tag{10}$$

Proof: See Appendix A.

According to the proposed model, devices in different tiers differ in the number of antennas and follow multiple mutually independent homogeneous PPPs. Therefore, the total SINR distribution of the mm-wave D2D network can be computed using the law of total probability as follows.

Corollary 1. *For the overall active user, the link success probability is*

$$P(\theta) = \sum\nolimits_{k\in[K]} \frac{\lambda_k q_k}{\sum_{i\in[K]} \lambda_i q_i} P_k(\theta). \tag{11}$$

Proof: Let us consider the point process of all active receivers (those who have active transmitters) and focus on the typical receiver of this point process. Based on Theorem 1, which gives the link success probability conditioned on this typical receiver belonging to the k-th tier, the overall link success probability is obtained as

$$P(\theta) = \sum\nolimits_{k\in[K]} \mathbb{P}(x \in \Phi_k) P_k(\theta), \tag{12}$$

where $\mathbb{P}(x \in \Phi_k)$ is the probability that the typical receiver belongs to the k-th tier. Since $\mathbb{P}(x \in \Phi_k) = \frac{\lambda_k q_k}{\sum_{i\in[K]}\lambda_i q_i}$, we obtain (11). ■

B. Bounds on Success Probability

Note that though the Laplace transform of the aggregate interference can be easily evaluated by numerical integration, the corresponding n-th derivative needs tedious and extensive computations, which makes the exact calculation inefficient. Thus, we obtain upper and lower bounds for the exact results by using bounds of the incomplete gamma functions.

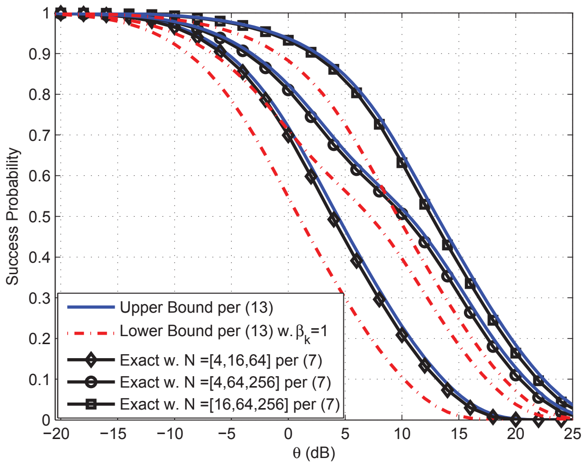

Fig. 2. The success probability for different configurations of antenna arrays.

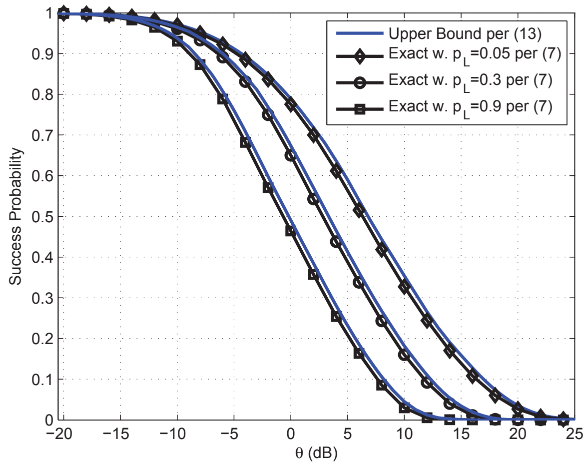

Fig. 3. The success probability for different LOS probabilities.

Theorem 2. *Let* $\beta_k = [\Gamma(1+M_{k,\mathrm{L}})]^{-1/M_{k,\mathrm{L}}}$ *and*

$$\hat{P}_k(\theta) = \sum_{m=1}^{M_{k,\mathrm{L}}} \binom{M_{k,\mathrm{L}}}{m} (-1)^{m+1} \mathcal{L}(u)\big|_{u=m\theta\beta_k\epsilon_k}. \quad (13)$$

For K-tier Poisson mm-wave D2D communication networks, the link success probability of the active device belonging to the k-th tier $P_k(\theta)$ is upper bounded by $\hat{P}_k(\theta)$, while a lower bound on $P_k(\theta)$, denoted by $\check{P}_k(\theta)$, is achieved by setting $\beta_k = 1$ in (13).

Proof: It is known from [10] that

$$1-[1-\exp(-x)]^M \le \widetilde{\Gamma}(M,x) \le 1-[1-\exp(-\beta x)]^M, \quad (14)$$

where $\beta = [\Gamma(1+M)]^{-1/M}$, $\widetilde{\Gamma}(M,x) = \Gamma(M,x)/\Gamma(M)$, and the equality holds only if $M = 1$. Based on this inequality, the lower and upper bounds on the link success probability are obtained as follows. Letting $\beta_k = [\Gamma(1+M_{k,\mathrm{L}})]^{-1/M_{k,\mathrm{L}}}$ and $\hat{P}_k(\theta)$ be the upper bound on $P_k(\theta)$, we have

$$\begin{aligned}\hat{P}_k(\theta) &= 1 - \mathbb{E}\left[\Big(1-\exp\big(-\theta\beta_k\epsilon_k(1+I)\big)\Big)^{M_{k,\mathrm{L}}}\right] \\ &= \sum_{m=1}^{M_{k,\mathrm{L}}} \binom{M_{k,\mathrm{L}}}{m} (-1)^{m+1} \mathbb{E}\Big[\exp\big(-m\theta\beta_k\epsilon_k(1+I)\big)\Big] \\ &= \sum_{m=1}^{M_{k,\mathrm{L}}} \binom{M_{k,\mathrm{L}}}{m} (-1)^{m+1} \mathcal{L}(u)\big|_{u=m\theta\beta_k\epsilon_k}. \quad (15)\end{aligned}$$

By substituting (8) into (15), we obtain the upper bound for the link success probability. From (14), the lower bound for the link success probability $\check{P}_k(\theta)$ is then obtained by setting $\beta_k = 1$ in (15). ∎

Remark 1. *Compared with the exact results for the SINR distribution, both bounds give much simpler expressions without requiring the derivatives for $\mathcal{L}(u)$ at $u \neq 0$, where $\mathcal{L}(u)$ is the product of multiple exponential functions with integral expressions in the exponents. Thus the effort for the computation of the SINR distribution is significantly reduced.*

Similar to the exact results, we can obtain bounds for the overall link success probability by Corollary 1.

IV. Numerical Results

In this section, we give some numerical results of the success probability for the heterogeneous mm-wave D2D networks, where $K = 3$, $\lambda_i = 0.1$, $\mu_i = 20$, $q_i = 1$, $\alpha_{i,\mathrm{L}} = 2.5$, $\alpha_{i,\mathrm{N}} = 4$, $M_{i,\mathrm{L}} = 4$, $M_{i,\mathrm{N}} = 2$, $i \in [K]$, $r_0 = 2$, $d_0 = 1$, $R = 200$ are default values.

Fig. 2 illustrates the success probability as a function of θ for different configurations of antenna arrays in a 3-tier mm-wave D2D network. It can be seen that the upper bound (13) derived for the success probability is quite tight, and the horizontal gap between the bounds and the exact curve is nearly constant, with the upper bound less than 0.5 dB and the lower bound about 2.2 dB away. Moreover, it is also observed that the configuration with larger antenna arrays performs better in terms of the success probability, since larger antenna arrays produce narrower transmission beams, which limit the interference signal to a certain direction, causing less interference to the receivers. Comparing the curves corresponding to the combinations of antenna arrays $[4, 64, 256]$ and $[16, 64, 256]$, there is a critical point at $\theta = 10$ dB, where the success probability with $[4, 64, 256]$ is quite close to but smaller than that with $[16, 64, 256]$. This is because when the SINR threshold is large, the successful transmissions mostly occur at the transmitters with larger antenna arrays (e.g., $N_3 = 256$). In this case, the desired signal between two cases is almost at the same level while the interference suffered in the case of $N = [4\ 64\ 256]$ is more severe than that in the case of $N = [16\ 64\ 256]$.

Fig. 3 shows the impact of LOS probability p_{L} on the success probability in a 3-tier mm-wave D2D network, where $N_1 = 4$, $N_2 = 16$, and $N_3 = 64$. It is observed that the link success probability deteriorates with the increase of p_{L}. The reason is that a high LOS probability means the propagation environment suffers from less blockage and, accordingly, the interfering signal experiences less propagation loss than that in the blocked case. As a result, the aggregate interference at receivers will become more severe, thereby decreasing the success probability.

V. Conclusion

In this paper, we analyzed the performance of mm-wave D2D networks where devices are diversified in their directional antenna arrays. Interestingly, we found that the first side lobe gain of a larger antenna array can be close to the main lobe gain of a smaller one merely in a limited spatial direction, and demonstrated that the mostly used sectored model cannot reflect this very important feature and thus is not suitable for mm-wave networks composed of increasingly diverse devices. In contrast, the cosine antenna pattern has superior accuracy and similar analytical tractability. By adopting this consine antenna pattern, we derived the success probability of the typical receiver and provided tight bounds to simplify the exact results. It was observed that the introduction of large antenna arrays in mm-wave networks bring immense benefits in terms of the success probability (reliability), which can not only improve the desired signal but also significantly reduce the interference. Overall, the results provide valuable engineering insights to help network operators deploy mm-wave D2D networks that satisfy stringent reliability requirements.

Acknowledgment

The work of N. Deng and Y. Sun has been supported by National Natural Science Foundation of China (61701071), Fundamental Research Funds for the Central Universities (DUT16RC(3)119), and the work of M. Haenggi has been supported by the U.S. NSF (grant CCF 1525904).

Appendix

A. Proof of Theorem 1

Proof: The link success probability of a device belonging to the k-th tier, denoted by $P_k(\theta)$, is expressed as

$$\begin{aligned} P_k(\theta) &= \mathbb{E}\left[\widetilde{\Gamma}\left(M_{k,\mathrm{L}}, \theta\epsilon_k(1+I)\right)\right] \\ &= \sum_{m=0}^{M_{k,\mathrm{L}}-1} \mathbb{E}\left[e^{-\theta\epsilon_k(1+I)}\frac{(\theta\epsilon_k(1+I))^m}{m!}\right] \\ &= \sum_{m=0}^{M_{k,\mathrm{L}}-1} \frac{(-u)^m}{m!}\mathcal{L}^{(m)}(u)|_{u=\theta\epsilon_k} \end{aligned}$$

where $\widetilde{\Gamma}(x,y) = \Gamma(x,y)/\Gamma(x)$ is the normalized incomplete gamma function, $\mathcal{L}(u) = \mathbb{E}[e^{-u(I+1)}]$ is the Laplace transform of the interference and noise, and the superscript (m) stands for the m-th derivative of $\mathcal{L}(u)$. Due to the independence of the K tiers, we have

$$\mathcal{L}(u) = e^{-u}\prod_{i\in[K]}\prod_{s\in\{\mathrm{L},\,\mathrm{N}\}}\mathcal{L}_{I_{i,s}}(u), \tag{16}$$

where $\mathcal{L}_{I_{i,s}}(u)$ follows as

$$\begin{aligned} &\mathcal{L}_{I_{i,s}}(u) = \mathbb{E}[\exp(-uI_{i,s})] \\ &= \mathbb{E}\left[\prod_{x\in\Phi_{i,s}}\left(\frac{q_i}{\left(1+u\mu_i G_i(\varphi_x)\ell_i(x)/M_{i,s}\right)^{M_{i,s}}}+1-q_i\right)\right] \\ &= \exp\left(-p_s\lambda_i q_i\frac{2}{N_i}\left(\pi R^2\right.\right. \\ &\left.\left. - \int_0^R\int_0^{\frac{\pi}{2}}\frac{4M_{i,s}^{M_{i,s}} r\mathrm{d}x\mathrm{d}r}{\left(M_{i,s}+u\mu_i N_i\cos^2 x\max\{r,d_0\}^{-\alpha_{i,s}}\right)^{M_{i,s}}}\right)\right). \end{aligned} \tag{17}$$

Letting $\mathcal{L}(u) = \exp(\eta(u))$ and thus $\mathcal{L}^{(1)}(u) = \eta^{(1)}(u)\mathcal{L}(u)$, $\mathcal{L}^{(m)}(u)$ can be calculated recursively according to the formula of Leibniz for the higher-order derivative of the product of two functions, given by

$$\mathcal{L}^{(m)}(u) = \frac{\mathrm{d}^{m-1}}{\mathrm{d}u}\mathcal{L}^{(1)}(u) = \sum_{n=0}^{m-1}\binom{m-1}{n}\eta^{(m-n)}(u)\mathcal{L}^{(n)}(u), \tag{18}$$

where the n-th derivative of $\eta(u)$ is easily given by (10). ■

References

[1] Cisco, "Cisco visual networking index: Global mobile data traffic forecast update, 2016-2021," http://www.cisco.com/c/en/us/solutions/collateral/service-provider/visual-networking-index-vni/mobile-white-paper-c11-520862.pdf, Feb. 2017.
[2] K. Venugopal, M. C. Valenti, and R. W. Heath, "Device-to-device millimeter wave communications: Interference, coverage, rate, and finite topologies," *IEEE Transactions on Wireless Communications*, vol. 15, no. 9, pp. 6175–6188, Sept 2016.
[3] X. Yu, J. Zhang, M. Haenggi, and K. B. Letaief, "Coverage analysis for millimeter wave networks: The impact of directional antenna arrays," *IEEE Journal on Selected Areas in Communications*, vol. 35, no. 7, pp. 1498–1512, July 2017.
[4] N. Deng and M. Haenggi, "A fine-grained analysis of millimeter-wave device-to-device networks," 2017, accepted at *IEEE Transactions on Communications*. Available on IEEE Xplore Early Access.
[5] M. Haenggi, *Stochastic geometry for wireless networks*. Cambridge University Press, 2012.
[6] S. Singh, M. N. Kulkarni, A. Ghosh, and J. G. Andrews, "Tractable model for rate in self-backhauled millimeter wave cellular networks," *IEEE Journal on Selected Areas in Communications*, vol. 33, no. 10, pp. 2196–2211, Oct 2015.
[7] J. G. Andrews, T. Bai, M. N. Kulkarni, A. Alkhateeb, A. K. Gupta, and R. W. Heath, "Modeling and analyzing millimeter wave cellular systems," *IEEE Transactions on Communications*, vol. 65, no. 1, pp. 403–430, Jan 2017.
[8] T. S. Rappaport, G. R. MacCartney, M. K. Samimi, and S. Sun, "Wide-band millimeter-wave propagation measurements and channel models for future wireless communication system design," *IEEE Transactions on Communications*, vol. 63, no. 9, pp. 3029–3056, Sept 2015.
[9] C. A. Balanis, *Antenna Theory: Analysis and Design*. Hoboken, NJ, USA: John Wiley & Sons, 2005.
[10] H. Alzer, "On some inequalities for the incomplete gamma function," *Mathematics of Computation*, vol. 66, no. 66, pp. 771–778, 1997.